The effect of composition, electron irradiation and quenching on ionic conductivity in a new solid polymer electrolyte: (PEG)$_x$NH$_4$I

R DAMLE[1,*], P N KULKARNI[1] and S V BHAT[2]

[1]Department of Physics, Bangalore University, Bangalore 560 056, India
[2]Department of Physics, Indian Institute of Science, Bangalore 560 012, India
*Corresponding author. E-mail: ramkrishnadamle@bub.ernet.in

Abstract. We have prepared, characterized and investigated a new PEG-2000 based solid polymer electrolyte (PEG)$_x$NH$_4$I. Ionic conductivity measurements have been made as a function of salt concentration as well as temperature in the range 265–330 K. Selected compositions of the electrolyte were exposed to a beam of 8 MeV electrons to an accumulated dose of 10 kGy to study the effect on ionic conductivity. The electrolyte samples were also quenched at liquid nitrogen temperature and conductivity measurements were made. The ionic conductivity at room temperature exhibits a characteristic double peak for the composition $x = 20$ and 70. Both electron beam irradiation and quenching at low temperature have resulted in an increase in conductivity by 1–2 orders of magnitude. The enhancement of conductivity upon irradiation and quenching is interpreted as due to an increase in amorphous region and decrease in crystallinity of the electrolyte. DSC and proton NMR measurements also support this conclusion.

1. Introduction

Ever since the first observation of high ionic conductivity in solid polymer electrolytes (SPE) in 1973, solvent-free polymer electrolytes have been an active topic of research [1,2]. SPEs have received considerable attention due to their valuable applications in high energy density batteries and electrochemical devices. A large number of SPEs have been studied till date [3]. Among these, poly(ethylene oxide) (PEO) has been widely studied as a host polymer complexed with alkali salts (lithium salt being the most studied) for use in all solid-state lithium batteries [4–8]. However, the disadvantage of these SPEs is the insufficient ionic conductivity although they have the advantage of most other properties being suitable for applications. Research and development are in constant progress in many ways to improve the ionic conductivity to attain a value $\sim 10^{-3}$ S/cm for practical use as

secondary lithium ion battery. Thus, the search for new SPEs and optimization of room temperature conductivity are still an active field of research. Ionic conductivity in SPEs can be improved either by lowering the glass transition temperature (T_g) of the polymer or by lowering the energy barrier for ionic movement. Several strategies have been suggested to achieve this which include (1) addition of plasticizers [9,10], (2) addition of nanosized ceramic fillers [11–15], (3) incorporating organic solvents [16], (4) exposure of SPEs to high energy ionizing radiation [17], (5) quenching at low temperature and (6) synthesizing new polymers or salts [18].

It is generally known that conductivity in SPEs is influenced by the concentration of defects and also the fraction of the amorphous region in the system [19]. Exposure of SPEs to high energy ionizing radiation has been tried out earlier to increase the amorphous content and decrease the crystallinity of the system [17].

Most of the studies of concentration and temperature dependence and enhancement of conductivity have been on high molecular weight host polymers. However, much attention has not been paid to the somewhat low molecular weight (MW ~2000) polymers. Shi and Vincent [20] have studied the effect of molecular weight of polymers on cation mobility and have shown that above a critical limit of 3200, the MW has no significant effect on cation mobility. However, below this limit, due to different viscosity and diffusion behaviours, an additional transport mechanism could be operating. In this low molecular weight region, referred to as the Rouse region, there is a possibility of the polymer chain diffusion besides the segmental motion. While PEO as host polymer complexed with alkali salts is well studied, there appears to be rather little focus on poly(ethylene glycol) (PEG) as a host polymer [21,22]. PEG has the same monomeric unit as PEO but has an end hydroxyl group, with the chemical formula: $H(-CH_2-CH_2-O-)_n-OH$.

Keeping these considerations in mind, we have synthesized, characterized and studied a new SPE $(PEG)_x NH_4 I$. We report here the effect of 8 MeV electron irradiation and quenching at low temperature on the ionic conductivity of $(PEG)_x NH_4 I$ polymer salt complex. The PEG (MW = 2000) used in our studies is a solid at room temperature with a melting point close to 50°C. It has 46 repeat units ($n = 46$) and is highly crystalline. NH_4^+ is a cation with small radius (1.4 Å), which is favourable for the polymer–salt complex formation. $NH_4 I$ is chosen as it fulfils the electrochemical stability criteria [6]. It has low lattice energy (637 kJ mol^{-1}) [23]. I^{-1} is a large soft anion having low charge density which would help in reducing the ion-pair formation with NH_4^+.

2. Experimental

The chemicals polyethylene glycol (PEG) of MW 2000 and $NH_4 I$ procured from Fluka were used without further purification. The $(PEG)_x NH_4 I$ complexes (in the composition $x = 15, 20, 30, 46, 70, 100, 150, 200, 300$ and 400 where x is the ratio of the number of ether oxygens in one monomer unit of the polymer to each NH_4^+ ion of the salt) were prepared by the standard solution cast method using methanol as the common solvent [24]. All the samples were dried under vacuum for several hours before using them for measurements. The X-ray diffraction (XRD) patterns were recorded using a Scintag XDS 2000 diffractometer at a scan rate of
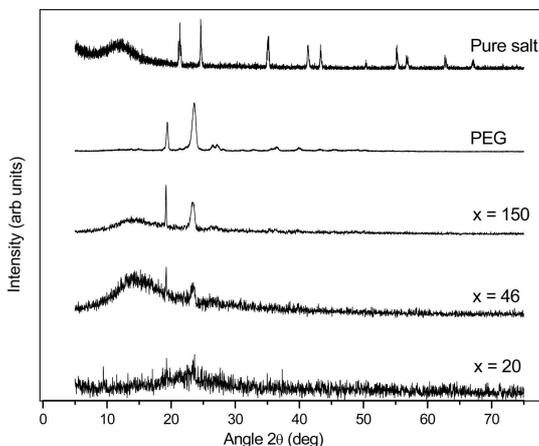
Figure 1. Powder XRD patterns of $(PEG)_x NH_4 I$.

$10°/$min. Differential scanning calorimetry (DSC) measurements were carried out on a MDSC 2920 (TA Instruments, USA) in standard mode. ^{1}H Nuclear magnetic resonance (NMR) linewidth measurements were carried out on a Bruker DSX-300 spectrometer operating at 300 MHz frequency. Ionic conductivity measurements were made using a dual phase lock-in-amplifier (PAR-5210) by the complex impedance method. To study the effect of ionizing radiation on ionic conductivity, selected compositions of the samples were exposed to a beam of 8 MeV electrons to an accumulated dose of 10 kGy and conductivity measurements were made immediately thereafter. Electron beam irradiation was carried out at Variable Energy Microtron Centre, Mangalore University, Mangalore, India. To study the effect of quenching, the samples were heated to its melting point of about 40–45°C and liquid nitrogen was poured on the molten sample. The rate of quenching was estimated to be about 20–25°C/s.

Since the samples with higher salt concentration are hygroscopic, there is a possibility of moisture contamination. Hence the samples were repeatedly dried under vacuum and repeated conductivity measurements were made to verify the reproducibility of the conductivity values. Consistence values of conductivity obtained after repeated vacuum drying rules out the possibility of water contamination. All the conductivity values are reported within an error margin of 5%.

3. Results and discussion

3.1 *XRD measurements*

XRD patterns (shown in figure 1) were recorded for a few salt compositions of the polymer–salt complexes, as well as that for pure PEG and pure $NH_4 I$ salt. Two prominent peaks of PEG (at $2\theta = 19.2$ and $23.4°$) are present in all the patterns indicating the presence of pure polymer in all. The $NH_4 I$ peaks are seen in none of the polymer–salt complexes indicating that $NH_4 I$ solvates well in PEG-2000
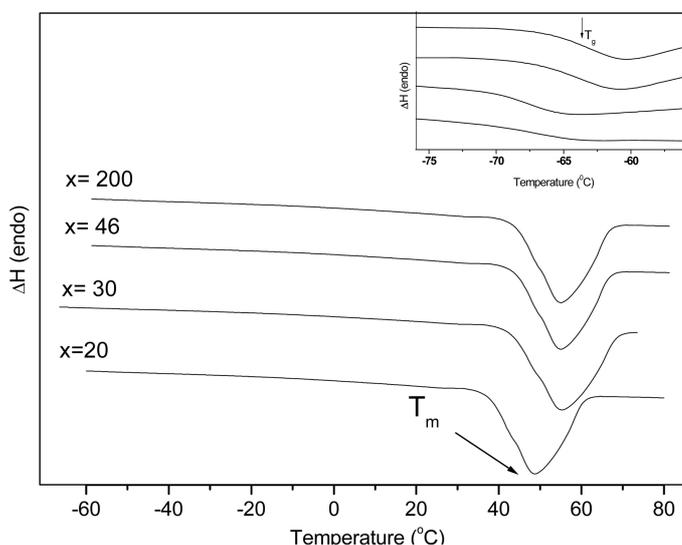
Figure 2. DSC traces (endothermic) of $(PEG)_x NH_4 I$. Inset shows the relevant regions magnified.

matrix. The intensity of the PEG peaks decreases at high salt concentrations. The diffraction peaks of the pure salt are absent in the polymer–salt complexes indicating the absence of pure salt phase in these complexes.

3.2 *DSC measurements*

Figure 2 shows the DSC curves (endothermic) registered for $(PEG)_x NH_4 I$ ($x = 15$, 46, 70 and 100). The summary of the DSC results for the heating cycle is given in table 1. An increase in the glass transition temperature T_g with an increase in the salt concentration was observed and this signifies that the flexibility of the polymer chains decreases with an increase in the salt concentration in the polymer system. This reduction in flexibility of chains is usually interpreted as being a result of the effects of an increase in intramolecular and intermolecular coordinations between coordinating sites on the same or different polymer chains caused by the ions acting as transient cross links [25]. Melting temperature T_m of SPE system decreases as the salt content increases.

The enthalpy of melting ΔH_m is less for the SPEs in comparison to that of pure PEG-2000. The area under the curve for the melting endotherm is related to the crystallinity of the specimen. The percentage or the degree of crystallinity X_c in the sample was estimated from the ratio of the enthalpy ΔH_m of the samples and the enthalpy of melting of 100% crystalline PEG ($\Delta H_m(PEG) = 202.41$ J/g [26]). X_c decreases as the salt concentration increases (table 1). With an increase in $NH_4 I$ salt concentration, ΔH_m decreases indicating a decrease in X_c [27]. Similar results have been obtained in $PEG_x LiClO_4$ SPE also [28]. The reduction in the crystalline fraction X_c with the increase in the salt concentration can be attributed to the inhibition of crystallization by the salt.

Table 1. DSC results of (PEG)$_x$NH$_4$I.

x	Salt in mole	T_m (°C)	T_g (°C)	ΔH_m (J/g)	% Crystallinity X_c
15	3.067	42.27	-62.80 ± 1.0	121.43	59.89
20	2.300	41.73	-64.26 ± 1.0	135.79	67.09
30	1.533	45.07	-62.40 ± 1.0	141.79	70.05
46	1.000	45.73	-60.55 ± 1.0	143.79	71.03
70	0.657	52.40	-59.80 ± 1.0	147.16	72.70
100	0.460	52.86	-63.00 ± 1.0	147.75	73.00
200	0.230	53.64	–	152.69	75.44
400	0.115	53.92	–	165.75	81.89
PEG	0.000	55.00	–	168.00	83.00

3.3 ^{1}H NMR results

The ^{1}H NMR spectra for low salt compositions ($x > 150$) and for pure PEG consist of two components, a strong broad signal and a relatively narrow and weaker signal superimposed on top of it (figure 3). While the polymer–salt complexes of lower salt concentration still show two overlapping signals, for complexes of higher salt concentration ($x < 150$), the broad component merges with the baseline. Other workers also have observed this feature earlier [29,30]. It is generally known that the broad component is due to the crystalline regions and the narrow component corresponds to the amorphous regions. A Gaussian curve fits to the broad signal and a Lorentzian to the narrow signal. Figure 4 shows the variation of ^{1}H NMR linewidth as a function of salt concentration. As the salt concentration increases, the linewidth decreases sharply in a similar way to the decrease in T_g as observed in DSC measurements and reaches a minimum at around $x = 20$ and then increases. Further increase in linewidth with salt concentration though X_c decreases could be due to the decrease in polymer chain flexibility as indicated by an increase in T_g at higher salt concentration. ^{1}H NMR signals for a few selected compositions of (PEG)$_x$NH$_4$I have been recorded as a function of temperature in the range 200–330 K. Figure 5 exhibits the variation of ^{1}H NMR linewidths as a function of temperature. From the linewidth data, correlation times τ_c's have been calculated using the equation [31]

$$\tau_c = \frac{1}{\alpha \pi \Delta \nu} \times \tan \left[\frac{\pi}{2} \times \left(\frac{(\Delta \nu)^2 - (\Delta \nu_r)^2}{(\Delta \nu_d)^2 - (\Delta \nu_r)^2} \right) \right], \tag{1}$$

where τ_c is the correlation time, α is a parameter of order unity, $\Delta \nu$ is the line width in the narrowing region (in Hz), $\Delta \nu_r$ is the residual linewidth and $\Delta \nu_d$ is the rigid lattice linewidth. τ_c's were calculated at various temperatures. From the slope of the $\ln(\tau_c)$ vs. $1000/T$ plot, E_a and τ_0 were estimated. The ionic conductivity σ_{NMR} was also calculated using the Nernst–Einstein relation
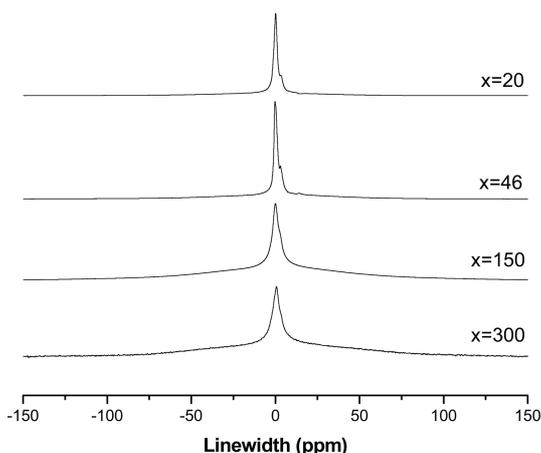
$$\sigma_{NMR} = \frac{N q^2 d^2}{6 \tau_c k T}, \tag{2}$$

Figure 3. Room temperature ^{1}H NMR signals of $(PEG)_x NH_4 I$ system, $x = 20$, 46, 150 and 300.

Table 2. Results of NMR parameters obtained from ^{1}H NMR linewidths for $(PEG)_x NH_4 I$.

x	τ_0 (s)	E_{aNMR} (eV)	τ_c at 300 K (s)	σ_{NMR} (S/cm)	σ (S/cm)
20	7.15×10^{-12}	0.254	6.53×10^{-7}	8.33×10^{-5}	4.77×10^{-6}
46	5.95×10^{-11}	0.296	1.10×10^{-6}	1.06×10^{-5}	2.63×10^{-6}
100	9.38×10^{-15}	0.520	5.14×10^{-6}	4.94×10^{-5}	4.78×10^{-6}

where N is the ammonium ion concentration per unit volume, d is the average ionic jump distance and q is the ionic charge. Considering an average interionic distance of $\sim 1.66 \pm 0.02$ Å, the value of N in $(PEG)_x NH_4 I$ can be calculated from the molecular weights and densities of PEG and $NH_4 I$ respectively, yielding $N \sim 1.4 \times 10^{26}$ m^{-3}. Activation energy $E_a(NMR)$ obtained from the plot of ln τ_c vs. $1000/T$ and hence σ_{NMR} calculated using eq. (2) are tabulated and compared with the values obtained from complex impedance spectroscopy in table 2. As seen from the table, σ_{NMR} is much higher than that measured from the complex impedance plot. Such discrepancies have been observed earlier in the literature. This could be due to the sensitivity of NMR to local dynamics in contrast with the conductivity measurement, which measures only the long-range transport. Another reason for this difference could be that while conductivity measurement responds to the motion of only charged (i.e., dissociated) species, NMR can sense the motion of undissociated molecules as well. Such differences in the conductivities determined by the two techniques have been discussed earlier [32].

3.4 *Ionic conductivity measurements*

The ionic conductivity as a function of salt concentration (mole fraction) for $(PEG)_x NH_4 I$ at 300 K is shown in figure 6. The conductivity isotherm shows
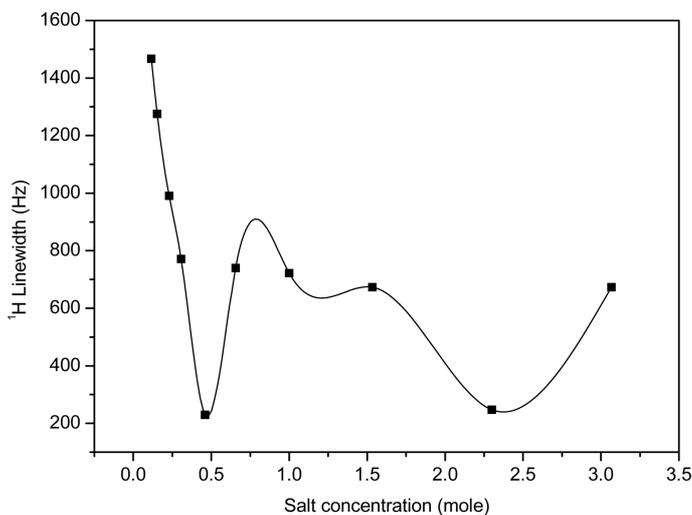
Figure 4. Room temperature ^{1}H NMR linewidths vs. salt concentration for $(PEG)_x NH_4 I$ system.
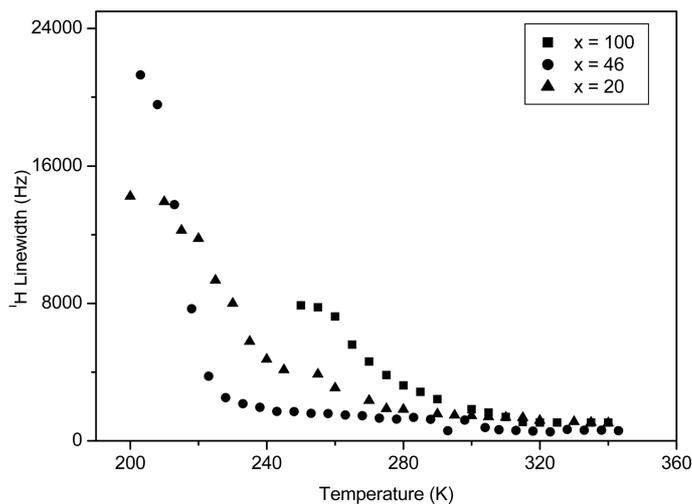

Figure 5. ^{1}H NMR linewidths vs. temperature plot for $(PEG)_x NH_4 I$ system.

a characteristic double peak for $x = 20$ and 70 with a conductivity maximum of about 4.7×10^{-6} S/cm. The initial increase in conductivity in the low concentration systems is explained as due to the increase in charge carriers as the number of free cations increases and also a decrease in X_c with an increase in salt concentration. The further decrease in σ though X_c decreases further at higher salt concentration could be due to an increase in the ion–ion interaction that impedes the motion of NH_4^+ and the stiffening of polymer chains as a result of cross-links formed by cations and salt precipitation [33]. Also, at higher salt concentration the formation
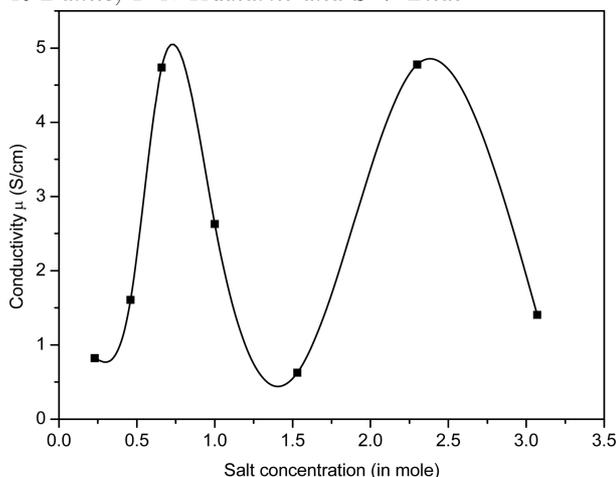
Figure 6. Variation of ionic conductivity with salt concentration in $(PEG)_x NH_4 I$ system.

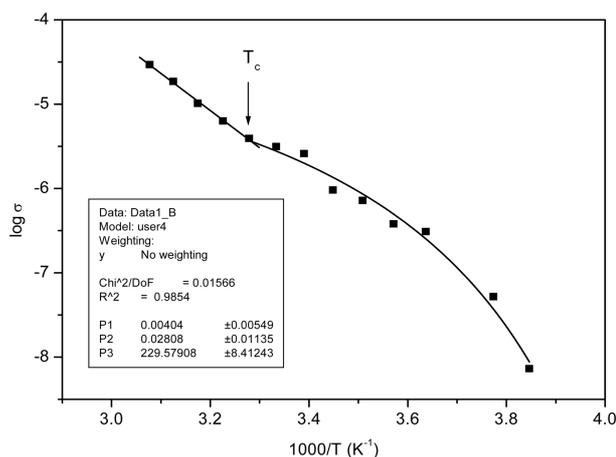**Figure 7.** Conductivity vs. temperature plot for $(PEG)_{20} NH_4 I$. The solid lines are fits to the Arrhenius (above T_c) and the VTF (below T_c) equations.

of ionic clusters too causes a decrease in mobility of charge carriers, since these large aggregates migrate slower than free ions because of their size. The observation of characteristic double peak in ionic conductivity has been well-established in the literature [34,35].

Ionic conductivity has also been measured as a function of temperature for a few selected compositions of the salt. Figure 7 shows the variation of conductivity as a function of temperature for $(PEG)_{20} NH_4 I$. The ionic conductivity increases monotonically as the temperature rises and reaches a high value $\sim 2.83 \times 10^{-4}$ S/cm at 330 K. From the temperature dependence experiments, it is seen that there exists a temperature T_c below which the conductivity plot has a curvature and above which it linearly and steeply raises till the melting temperature of the sample. The
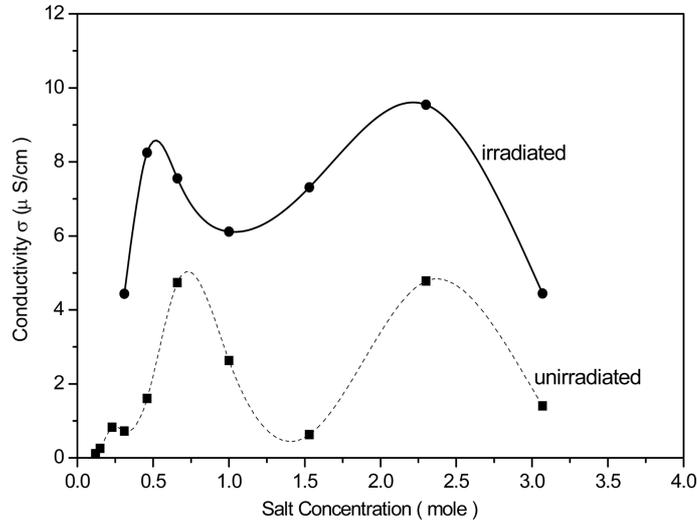
Figure 8. Ionic conductivity vs. salt concentration before and after electron beam irradiation in (PEG)$_x$NH$_4$I system.
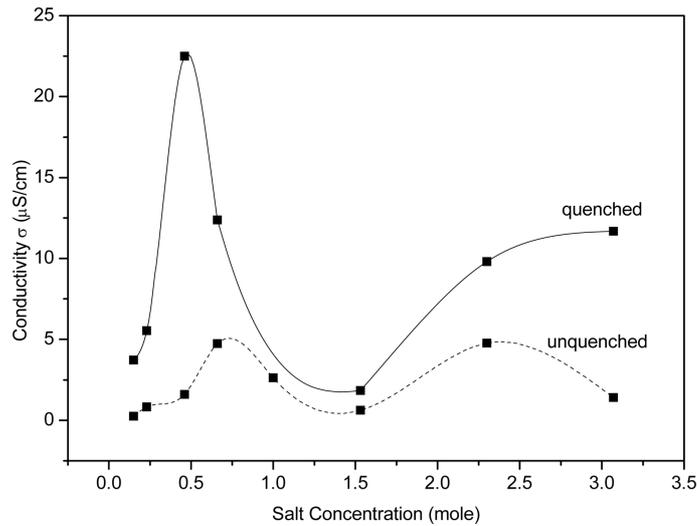

Figure 9. Ionic conductivity vs. salt concentration for (PEG)$_x$NH$_4$I system before and after quenching.

region below T_c fits the empirical Vogel–Tamman–Fulcher (VTF) [36–38] equation

$$\sigma = \frac{A}{\sqrt{T}} \exp\left(\frac{-B}{k(T - T_0)}\right), \tag{3}$$

where T is the absolute temperature and T_0 the ideal glass transition temperature that is usually 30–50° below T_g (it is the temperature at which the configurational
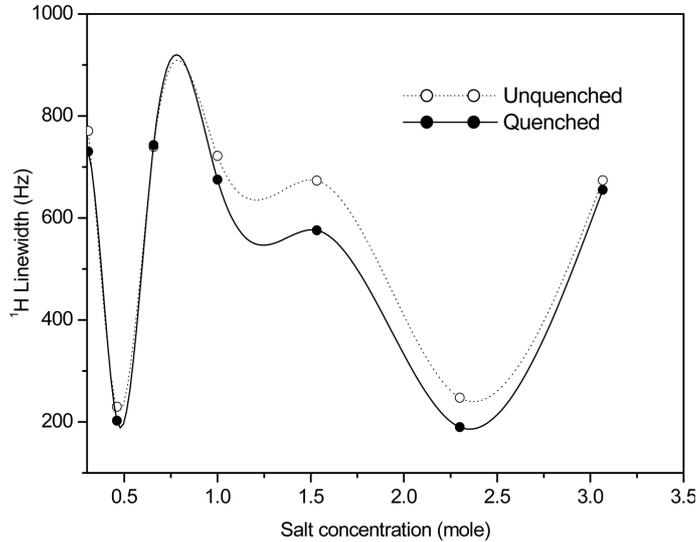
Figure 10. ^{1}H NMR linewidth as a function of salt concentration for $(PEG)_x NH_4 I$ before and after quenching.

Table 3. Arrhenius and VTF equations fitting parameters for $(PEG)_{20}NH_4I$.

x	Salt in mole	E_a (eV)	T_c (K)	A (SK$^{0.5}$ cm^{-1})	B (eV)	T_0 (K)
20	2.300	0.875	304	0.004	0.028	229.58

entropy vanishes), B is an apparent activation energy which is dependent on the free energy barrier opposing configurational rearrangements and A is a pre-exponential factor related to the number of carriers [39]. The fitting parameter values are given in table 3. The Arrhenius equation

$$\sigma = \sigma_0 \exp\left(\frac{-E_a}{kT}\right) \tag{4}$$

(where the symbols have their usual meanings) fits the region above T_c. The cross-over between Arrhenius and VTF behaviour of $\sigma(T)$ is widely reported and discussed in [4,40].

3.5 *Effect of electron irradiation on ionic conductivity*

Figure 8 shows the observed conductivity changes as a function of salt concentration before and after electron irradiation in $(PEG)_x NH_4 I$ system. Irradiating with 8 MeV electron beam has resulted in the increase in the ionic conductivity by nearly one order. The increase in conductivity is seen in almost all salt compositions. However, the increase is more pronounced in the medium salt concentration

Table 4. DSC results of quenched (PEG)$_x$NH$_4$I.

x	Salt content in mole	T_m (°C)		T_g (°C)		% Crystallinity	
		Unquenched	Quenched	Unquenched	Quenched	Unquenched	Quenched
15	3.067	42.3	50.4	−62.80	−60.9	59.89	47.03
20	2.300	41.7	51.5	−64.26	−45.3	67.09	46.13
30	1.533	45.1	50.7	−62.40	−45.3	70.05	49.41
46	1.000	45.7	51.5	−60.54	−	71.03	51.05
70	0.657	52.4	52.8	−46.40	−49.7	72.70	56.92
100	0.460	55.9	54.1	−58.65	−49.3	73.00	58.53
150	0.307	52.8	−	−	−	75.44	62.76
200	0.230	54.2	54.3	−	−	81.89	71.18
300	0.153	−	−	−	−	−	−
400	0.115	54.4	54.8	−	−	−	−
PEG	0.000	55.0	−	−	−	168.00	−

range $x = 20$ and 100. The maximum conductivity achieved after irradiation is 9.63×10^{-6} S/cm for $x = 20$. The increase in conductivity after electron beam irradiation could be due to the increase in the amorphous content of the sample. The electrolyte samples were irradiated by 8 MeV electrons to three different doses (5, 10 and 15 kGy) and conductivity measurements were made. Ionic conductivity is found to increase by the same order after each accumulated dose. However, maximum enhancement in conductivity is observed after irradiation to an intermediate dose of 10 kGy. The results are thus reported only for the dose of 10 kGy. Conductivity measurements were carried out over a period ranging from a few hours to several months after irradiation. The observation is that there is hardly any change in the values of conductivity. This would indicate that the irradiation-induced effects are permanent in nature.

3.6 *Effect of quenching on ionic conductivity*

Figure 9 depicts the observed conductivity changes as a function of salt concentration before and after quenching. The process of quenching enhances the ionic conductivity by one to two orders of magnitudes. It is observed that the conductivity enhancement is seen in all salt compositions. The maximum conductivity after quenching is found to be 2.26×10^{-5} S/cm for $x = 100$. Table 4 shows the DSC results obtained before and after quenching. The percentage of crystallinity is found to decrease in almost all salt compositions after quenching. The DSC studies reveal that increase in the conductivity is more due to the increase in the amorphous content (or decrease in crystallinity) of the system after quenching. ^{1}H NMR linewidths were also recorded at room temperature for both quenched and unquenched systems (figure 10). The process of quenching is found to decrease the linewidth marginally. The lowest linewidth is observed for $x = 100$ concentration, for which the quenching process has shown maximum enhancement in ionic conductivity.

4. Conclusions

A new solid polymer electrolyte $(PEG)_x NH_4 I$ were synthesized, characterized and studied using XRD, DSC, NMR and AC conductivity techniques. XRD results confirm the formation of polymer–salt complex. The samples with higher salt concentrations are softer and moderately hygroscopic. Samples of intermediate salt concentrations are less hygroscopic and show higher ionic conductivity. The room temperature conductivity is highest (4.78×10^{-6} S/cm) for $x = 20$ and 70. At low salt concentrations they are highly crystalline and less hygroscopic and have moderate room temperature conductivity of the order of 10^{-7} S/cm. As the salt concentration increases they become more amorphous leading to increase in conductivity. The concentration dependence of conductivity shows characteristic peaks for intermediate salt concentration ($x = 20$ and 70). The glass transition temperature is minimum for intermediate salt concentration ($x = 20$) and for all other salt concentrations T_g is higher due to stiffening of the polymer chains due to cross-linking among them. T_m of samples is lower than the pure PEG-2000. The degree of crystallinity X_c is observed to decrease with an increase in salt concentration. This reduction in X_c is attributed to the lower T_m and decrease in heat of melting ΔH_m with the increase in salt concentration. ^{1}H NMR linewidths and DSC results are consistent with the room temperature conductivity results. The ionic conductivity increases monotonically with temperature and reaches a maximum value of 2.83×10^{-4} S/cm at temperature 330 K. The temperature dependence of conductivity fits the Arrhenius and VTF equations at different temperature ranges.

The process of exposing the solid polymer electrolytes to electron beam and also quenching to liquid nitrogen temperature gives rise to an increase in conductivity by nearly one order of magnitude. Exposure of the present polymer electrolytes to electron beam may have resulted in the increase in the amorphous fraction of the complex and hence decrease in the degree of crystallinity. Of the two methods of conductivity enhancement, quenching appears to be more effective giving rise to a maximum conductivity of 2.26×10^{-5} S/cm for $x = 100$.

The radiation damage in polymer electrolyte is also known to cause chain scission (fragmentation) and cross-linking. Chain scission leads to a higher flexibility of polymer chains. Cross-linking leads to a decrease in the flexibility of polymer segments (resulting in a decrease in conductivity). Perhaps in the present system, irradiation may also has resulted in chain scission resulting in the increase in the flexibility of polymer chains and hence the conductivity enhancement. Thus, irradiation of SPEs by ionizing radiation and also quenching at low temperature appear to be promising methods to enhance ionic conductivity in known solid polymer electrolytes.

Acknowledgements

References

[1] D E Fenton, J M Parker and P V Write, *Polymer* **14**, 589 (1973)
[2] P V Write, *Br. Polym. J.* **7**, 319 (1975)
[3] V Chandrashekar, in: *Advances in polymer science* edited by S Edwards (Springer Verlag, Berlin, 1996) Vol. 135, pp. 139–205
[4] A Ratner, in: *Polymer electrolytes reviews* edited by J R MacCallum and C A Vincent (Elsevier Appl. Sci. London, 1987 and 1989), Vol. 1 and 2
[5] M B Armand, *Ann. Rev. Mater. Sci.* **16**, 245 (1986)
[6] C A Vincent, *Prog. Solid State Chem.* **17**, 145 (1987)
[7] M Watanabe and N Ogata, *Br. Polym. J.* **17**, 145 (1988)
[8] M A Ratner and D F Shriver, *Chem. Rev.* **88**, 109 (1988)
[9] R Hug, G C Farrington, R Koksbang and P E Tonder, *Solid State Ionics* **57**, 277 (1992)
[10] A M Sukeshini, A R Kulkarni and A Sharma, *Solid State Ionics* **113–115**, 179 (1998)
[11] F Croce, G B Appetecchi, L Persi and B Scrosati, *Nature (London)* **394**, 456 (1998)
[12] H Sun, H J Sohn, O Yamatomo, Y Takeda and N Imanishi, *J. Electrochem. Soc.* **146**, 1672 (1999)
[13] Th Joykumar Singh, T Mimani, K C Patil and S V Bhat, *Solid State Ionics* **154–155**, 21 (2002)
[14] Th Joykumar Singh and S V Bhat, *J. Power Sources* **129**, 280 (2004)
[15] Joykumar S Thokchom, Christina Chen, K M Abraham and Binod Kumar, *Solid State Ionics* **176**, 1887 (2005)
[16] A G Bishop, D R MacFarlance, McNaughton and M Forsyth, *J. Phys. Chem.* **11**, 2237 (1996)
[17] Th Joykumar Singh, Ganesh Sanjeev, K Siddappa and S V Bhat, *J. Polym. Sci. Part B: Polym. Phys.* **42**, 1299 (2004)
[18] W H Meyer, *Adv. Mater.* **102**, 352 (1998)
[19] C Berthier, W Gorecki, M Minier, M B Armand, J M Chabagno and P Rigaud, *Solid State Ionics* **11**, 91 (1983)
[20] J Shi and C A Vincent, *Solid State Ionics* **60**, 11 (1993)
[21] R K Gupta, H Y Jung and C M Whang, *J. Mater. Chem.* **12**, 3779 (2002)
[22] Y Kato, K Hasumi, S Yokoyama, T Yabe, H Ikuta, Y Uchimoto and M J Wakihara, *Thermal Analysis and Calorimetry* **69**, 889 (2002)
[23] H D B Jenkins and D F C Morris, *Mol. Phys.* **32(1)**, 231 (1976)
[24] Nader Binesh and S V Bhat, *Solid State Ionics* **92**, 261 (1996)
[25] J F Le Nest, A Gandini and H Cheradane, *Br. Polym. J.* **20**, 253 (1988)
[26] X Li and S L Hsu, *J. Polym. Sci., Polym. Phys. Ed.* **22**, 1331 (1984)
[27] M Watanabe, M Togo, K Sanui, N Ogata, T Kobayashi and Z Ohtaki, *Macromolecules* **17**, 2908 (1984)
[28] T Joykumar Singh and S V Bhat, *Bull. Mater. Sci.* **26**, 707 (2003)
[29] K Hikichi and J Furuichi, *J. Polym. Sci.* **A3**, 3003 (1965)
[30] A Johansson, A Wendsjö and Tegenfeldt, *J. Electrochim. Acta* **37**, 1487 (1992)
[31] J R Hendrickson and P J Bray, *J. Magnetic Resonance* **9**, 341 (1973)
[32] D Brinkmann, *Progress in NMR Spectroscopy* **24**, 527 (1992).

[33] F M Gray, *Solid polymer electrolyte – Fundamentals and technological applications* (VCH Inc., New York, 1991)
[34] F M Gray, *Solid State Ionics* **40–41**, 637 (1990)
[35] C D Robitaille and D Fauteux, *J. Electrochem. Soc.* **133**, 315 (1986)
[36] H Vogel, *Phys.* **Z22**, 645 (1922)
[37] V G Tamman and H Z Hesse, *Anorg. Allg. Chem.* **19**, 245 (1926)
[38] G H Fulcher, *J. Am. Ceram. Soc.* **8**, 339 (1925)
[39] J H Gibbs and E A DiMarzio, *J. Chem. Phys.* **28**, 373 (1958)
[40] N Binesh and S V Bhat, *J. Polym. Sci. Part B: Polym. Phys.* **36**, 1201 (1998)